A Method for Measuring Interface Roughness from Cross-Sectional Micrographs

Shreyas Balachandran, David B. Smathers, Jiman Kim, Kihong Sim, and Peter J. Lee, *Senior Member, IEEE*

***Abstract*—Uniform co-deformation of Nb, Ta, and their alloys in a Cu matrix is vital for performance yield for most internal-Sn Nb_3Sn conductors, however, multiple factors can result in instabilities during extrusion and drawing. A better understanding of the variability can be attained by quantifying the interface roughness, however, there has been no consistent method developed to do this. Here we present a method to derive traditional stylus-based roughness measurements, including root-mean-square and average roughness values from micrographs of curved interfaces by image and signal processing analysis. Deformation creates interface roughness with different wavelengths. The longer wavelength or waviness and shorter wavelength or roughness are separated in this method. We apply the technique to 12 different commercial Nb filaments drawn in a Cu matrix. We find good correspondence between the roughness and initial Nb grain size of the rods. The procedure developed has been made available with the open-source code made available to the community. The procedure developed could be used to optimize the wire architecture for next-generation high-field magnets that use Nb alloys.**

***Index Terms*—Superconducting filaments, superconducting wires.**

I. Introduction

NB_3SN is one of the most mature conductors for next-generation accelerator magnets and is a prime candidate for a future circular collider (FCC) [1]. The challenging target specifications [2] require further optimization of Nb_3Sn conductor designs, which need Nb alloys to be drawn effectively in a Cu matrix to large strains to achieve smaller d_{eff}. An issue with drawing Nb (which is body-centered cubic), in a Cu (which is face-centered cubic) matrix, and Nb and Cu being immiscible in all temperature ranges, is the creation of a well-defined but jagged interface. This high interface roughness can play a significant role in conductor breaks (filaments are drawn to engineering strains greater than 15 during the wire-drawing process), [3] and in some architectures merging of filaments during the reaction heat treatment process results in higher losses [4], [5]. The magnitude of the interface roughness can be decreased by control of the initial Nb alloy grain size [6], [7]. An average starting Nb alloy grain size of less than 50 μm (<ASTM 5.5) is preferred by wire manufacturers to reduce the interface roughness.

Manuscript received 21 November 2022; revised 3 February 2023; accepted 20 February 2023. Date of publication 6 March 2023; date of current version 10 March 2023. This work was supported in part by the State of Florida, Florida State University, in part NSF Cooperative Agreement DMR-1644779 and the State of Florida at the NHMFL. *(Corresponding author: Peter J. Lee.)*

Shreyas Balachandran was with the Applied Superconductivity Center, National High Magnetic Field Laboratory, Tallahassee, FL 32310 USA, and also with the Florida State University, Tallahassee, FL 32306 USA. He is now with the Jefferson Lab, Newport News, VA 23606 USA.

David B. Smathers is with the Materion, Mayfield Heights, OH 44124 USA.

Jiman Kim and Kihong Sim are with the Kiswire Advanced Technology, Company Ltd, Daejeon 34026, South Korea.

Peter J. Lee is with the Applied Superconductivity Center, National High Magnetic Laboratory, Tallahassee, FL 32310 USA, and also with the Florida State University, Tallahassee, FL 32306 USA (e-mail: lee@asc.magnet.fsu.edu).

Color versions of one or more figures in this article are available at https://doi.org/10.1109/TASC.2023.3250165.

Digital Object Identifier 10.1109/TASC.2023.3250165

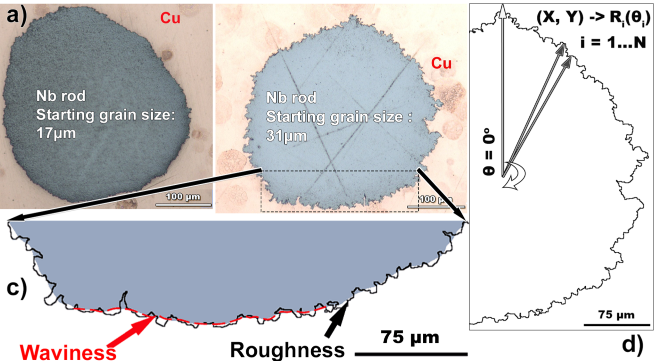

Fig. 1. Light microscope images of transverse cross-sections at an intermediate processing step of two Nb filaments drawn in a Cu matrix (internal-tin Nb_3Sn conductor fabricated by KAT). The interface roughness appears to be smaller in Nb filament (a) with an average starting grain size of 17 μm versus (b) with an initial grain size of 31 μm. (c) The interfacial topography can be separated into components with a longer wavelength, referred to as waviness (dashed red line), and a shorter wavelength, called roughness (solid black line). (d) Outline of the Nb rod: The centroid of the shape and the interface can be extracted using macros in Fiji. All the interface (X,Y) points can transformed to R (θ).

Recently, Smathers et al. [8] have been able to correlate the wire performance to the initial starting grain size by measuring the critical current, I_c, and AC losses in the conductor fabricated by KAT. With all the grain sizes being less than ASTM 6, there are still variations in the interface roughness, and the results suggest that AC losses in the conductor may correlate to the interface roughness. For optimization of conductor designs for next-generation conductors quantifying interface roughness provides a decision metric.

Fig. 1 shows two Nb filaments in a Cu matrix, with average starting grain sizes of 17 μm and 31 μm, showing the interface roughening. As indicated in Fig. 1(c), the Nb interface consists of two different wavelengths: the longer wavelength, called waviness, and the shorter wavelength, roughness. The terminology is by EN-ISO 4287 [9]. In addition to different wavelengths, the curved shape and embedded nature of the filaments make stylus-based methods challenging. In this paper, we provide a

1051-8223 © 2023 IEEE. Personal use is permitted, but republication/redistribution requires IEEE permission.
See https://www.ieee.org/publications/rights/index.html for more information.

Authorized licensed use limited to: Florida State University. Downloaded on June 28,2023 at 15:27:21 UTC from IEEE Xplore. Restrictions apply.

method that can be used to quantify the interface roughness for curved shapes, such as filaments using cross-sectional microscopy images. Here, we develop a process and apply this technique to multifilamentary wires that were drawn by KAT which have starting Nb grain size between 15-40 μm. We find that there are tractable variations in Cu: Nb interface roughness.

Most image analysis techniques for surface texture and roughness measurements have employed fractal analysis, a complete review of these methods is outlined in the following reference [10]. The process developed here is for continuous curves and is applicable for planar and curved surfaces. A similar image analysis method for roughness characterization of planar interfaces has been performed before [11], [12]. The article extends image analysis techniques for roughness characterization for high curvature surfaces. Validation of the method using a stylus based physical measurement is challenging for such interfaces and beyond the scope of this paper.

II. Methods

A. Description of Samples Used in This Study

The sample micrographs used in this study are of Nb filaments in a Cu matrix provided by KAT as a part of their ongoing distributed-Sn Nb_3Sn wire development for the Divertor Test Tokamak (DTT) facility. The micrographs are from the production batch of Nb_3Sn wire for DTT at an intermediate stage of wire drawing. The starting grain sizes of the Nb rods before any wire drawing varied between 20 μm and 40 μm. The strain of the Nb rods is proprietary information and was not disclosed. Details of wire fabrication and superconducting testing are presented elsewhere [8].

B. Image Processing Using ImageJ

ImageJ, an open-source software developed by NIH [13], is used to convert the original light microscope images of the filament cross-sections into a binary image of the interface that can then be quantified. The pixel size of ~400 nm in these images provides a lower bound to these measurements. Sequential pixel locations along the interface are identified using a script (github.com/peterjlee/asc-ImageJ-Unravel) written in the ImageJ macro language. To measure the interface roughness a reference needs to be established. For a flat profile, the reference would be a straight line and the roughness (r) would be a measure of deviation from that line. However, for curved shapes as the micrograph in Fig. 1(b), the reference needs to be established. Since the Nb alloy rods are initially circular, there is a physical basis to consider deviations from a circle or an ellipse (as they are deformed). For this analysis, deviations from a circle are employed, but the method is applicable for ellipses, polynomial fits, or a smoothed median interface as required by the interface that is being analyzed.

The points on the interface (X_i, Y_i) of the binary Fig. can be converted into polar coordinates $\mathrm{R_i}(\theta)$, as shown in Fig. 1(d), using the center of the object as the origin. The radial distances can be offset by subtracting the minimum distance in the set: $S(i) = R_i\text{-}R_{min}$. The raw signal, S, is a combination of the long wavelength, waviness (w), and short wavelength roughness (r).

C. Analysis of Profile Using Gwyddion

To deconvolute S into w and r we use the same ImageJ script to export a pseudo height map that can be imported into the widely used open-source topographic analysis software Gwyddion [14]. The steps taken to deconvolute the signal involve: a) choosing a cut-off wavelength, b) separating the signal into waviness based on the cut-off wavelength (λ) and roughness (r), c) traditional roughness measurement calculation, average roughness (R_a), and root mean square (rms) roughness (R_q).

$$R_a = \sum_{i=1}^{n} |r_i| \Bigg|, \; R_q = \sum_{i=1}^{n} |r_i^2| \Bigg| \; \mathrm{R_a} = \sum_{\mathrm{i=1}}^{\mathrm{n}} |\mathrm{r_i}| \Bigg|, \; \mathrm{R_q} = \sum_{\mathrm{i=1}}^{\mathrm{n}} |\mathrm{r_i^2}| \Bigg| \tag{1}$$

The waviness (w) calculations also involve an average waviness (W_a), and rms waviness (W_q).

$$W_a = \sum_{i=1}^{n} |w_i| \Bigg|, \; W_q = \sum_{i=1}^{n} |w_i^2| \Bigg| \; \mathrm{W_a} = \sum_{\mathrm{i=1}}^{\mathrm{n}} |\mathrm{w_i}| \Bigg|, \; \mathrm{W_q} = \sum_{\mathrm{i=1}}^{\mathrm{n}} |\mathrm{w_i^2}| \Bigg| \tag{2}$$

For the analysis of signal S, from Fig. 3, the correct choice of cut-off wavelength (λ_c) is crucial to separate w, and r.

D. Cut-Off Wavelength (λ_c, μm)

The one-dimensional texture is split into waviness (the low-frequency components defining the overall shape) and roughness (the high-frequency components) at the cut-off frequency. The cut-off frequency is related to the Nyquist frequency ($\mathrm{N_f}$), and a N_f of 1.0 corresponds to the frequency where all the spatial information of the signal is preserved and corresponds to the entire signal. To separate the waviness from the noise, a frequency analysis needs to be performed. For this paper, we will report the cut-off wavelength (λ_c, μm) since the measurements are in terms of length rather than time.

For the same signal in Fig. 2, if we deconvolute the signal into roughness and waviness, we observe that the value of R_a, R_q vary depending on the choice of λ_c as observed in Fig. 4. For instance, a λ_c of 500 μm samples the signal at a higher wavelength (lower frequency) which leads to a low roughness value as described by $R_a = 6.33$ μm, and $R_q = 7.72$ μm. Whereas, a λ_c of 10 μm produces sampling of the signal at a lower wavelength (higher frequency) and the generated roughness value is significantly higher: $R_a = 0.623$ μm, and $R_q = 0.783$ μm.

An appropriate λ_c needs to be chosen based on the characteristic feature lengths in the dataset. Fig. 2(a) and (b), contrast the waviness and roughness components generated using λ_c values of 500 μm and 10 μm respectively (in this instance we would expect a spatial resolution not lower than 1 μm). Plotting the dependence of roughness on chosen λ_c (Fig. 3) we observed an

Authorized licensed use limited to: Florida State University. Downloaded on June 28,2023 at 15:27:21 UTC from IEEE Xplore. Restrictions apply.

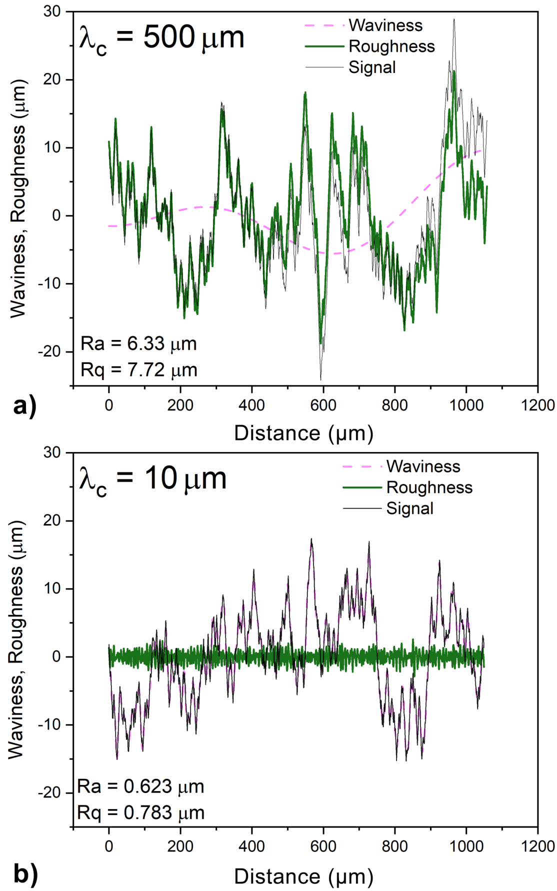

Fig. 2. Contrasting waviness and roughness extracted from the PHM signal using long and short values of cut-off wavelength: $\lambda_c =$ a) 500 μm, b) 10 μm.

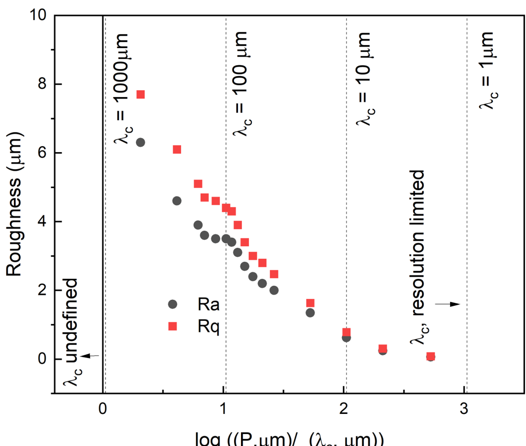

Fig. 3. Dependence of roughness values, R_a and R_q on chosen λ_c. Physical roughness is limited by the resolution of the image, the pixel size here is 400 nm, and any roughness value around 400 nm could be interpreted as noise.

inflection at a λ_c of $\sim$100 μm, representing a bifurcation in terms of waviness and roughness. The separation of waviness and roughness components for $\lambda_c =$ 100 μm is presented in Fig. 4, the R_a and R_q values are 3.61 μm, and 4.52 μm, respectively.

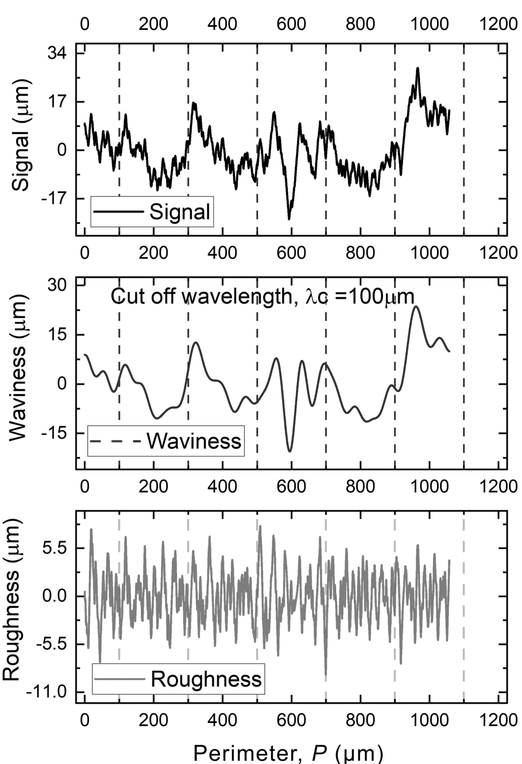

Fig. 4. Waviness and roughness extracted from the PHM signal, for $\lambda_c = 100$ μm.

We determine that a λ_c of 100 μm is suitable for these light micrographs of Cu-Nb filaments. It is essential to evaluate λ_c consistently for the data set that is being processed. A guide to choosing the cut-off wavelength could be 10–100 times the spatial resolution of the image. More work would be needed to obtain specific correlations to physical geometry-based parameters and sample dimensions.

E. Geometric Measures

The Cu-Nb interface roughness is caused by deformation; hence a complete description of the geometry of the Nb filaments is included for completeness. Quantitative image analysis in ImageJ also provides geometric measures of Area (A), Perimeter (P), major and minor elliptical-fit axes, and circularity (C). C is defined as the ratio: $4\pi A/P^2$. $C = 1$ for a circle, with values decreasing for increasing distortion. The aspect ratio (AR) measures the shear strain applied to the filament and is defined as a ratio: $AR =$ Major axis/Minor Axis. The higher the AR, the worse the overall macroscopic deformation.

III. Results and Discussion

A. Variation in Roughness Concerning Initial Grain Size

Table I compares the results of the image analysis with the wire properties. Fig. 5(a) shows the positive correlation between grain size and roughness (R_a, and R_q). These results suggest that the method developed here can capture the deformation of the interface region. The roughness scaling with Nb grain

Authorized licensed use limited to: Florida State University. Downloaded on June 28,2023 at 15:27:21 UTC from IEEE Xplore. Restrictions apply.

TABLE I
SUMMARY OF INTERFACE ROUGHNESS (R), WAVINESS (W) AND MEASURED PROPERTIES OF THE NB FILAMENTS AND WIRES IN THIS STUDY

ID‡	ASTM Number	Grain size + µm	R_a µm	R_q µm	W_a µm	W_q µm	Perimeter (P) µm	Major ellipse axis µm	Minor ellipse axis µm	Area (A) µm²	Circularity (C)	AR	±3 T Loss mJ/cm³	J_c(12 T, 4.2 K) A/mm²
134B_85a	8.5	19	1.2	1.6	5.5	7.2	1366	348	332	90726	0.6	1.05	791	1354
134B_85b			1.3	1.6	8.5	10.7	1340	361	321	91231	0.6	1.12		
158B_67a	6.7	35	3.5	4.5	6.0	7.5	1942	352	331	91573	0.3	1.06	834	1235
158B_67b			2.9	3.6	8.0	9.4	1906	343	338	91073	0.3	1.01		
156B_73a	7.3	29	2.7	3.4	5.5	6.7	1890	342	329	88384	0.3	1.04	852.6	1269
156B_73b			2.6	3.2	5.5	7.0	1923	360	328	92710	0.3	1.10		
165B_75a	7.5	27	2.3	2.8	6.1	7.5	1755	353	328	91071	0.4	1.08	762	1316
165B_75b			1.7	2.1	5.9	6.9	1498	351	339	93505	0.5	1.04		
166T_77a	7.7	25	1.7	2.2	5.4	7.1	1570	348	328	89780	0.5	1.06	663.3	1303
166T_77b			2.0	2.4	9.2	10.0	1716	342	334	89910	0.4	1.02		
173T_81a	8.1	22	1.7	2.2	3.6	4.3	1377	341	324	86741	0.6	1.05	608.5	1301
173T_81b			1.6	2.0	3.2	4.0	1296	340	333	89036	0.7	1.02		

+ Grain size in µm was calculated from the ASTM Number by: $254/(2_{N-1})_{1/2}$, where N = ASTM Number. ‡ The ID "a", "b" suffixes denote different filament micrographs from the same wire.

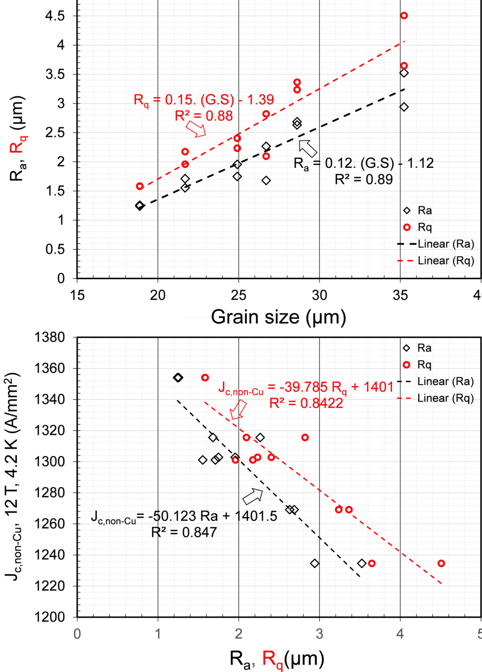

Fig. 5. (a) Roughness as a function of grain size, and (b) J_c as a function of roughness for all 12 filaments in this study. Least-square fits and their R^2 value are shown as a guide.

size is expected from the local grain level BCC plane strain deformation of Nb grains imposing on the softer FCC Cu matrix. An interpretation of the result could also be that a variation of R_a or R_q (whichever is greater) can be expected with the filament deformation. Initial Nb grain size could limit the spacing between Nb rods. According to the linear fit, an initial grain size of 10 μm would lead to a $R_a \approx 0.1$ μm, and $R_q \approx 0.11$ μm. It would be useful to extend this study to smaller filament diameters as the wire is drawn down and observe the trend.

B. Variation in Waviness Concerning Initial Grain Size

We did not observe any relationship between waviness and grain size. In principle, it can be contemplated that the waviness captures certain aspects of the macroscopic deformation, which could depend on the location of the Nb filaments in the stack. Variations in waviness as a function of strain could be a better parameter to track. In the filaments analyzed the variance in the areas of all the filaments is less than 2%. The aspect ratio of the filaments does not indicate any significant issues indicating that in the grain size range explored here, there are no instabilities in the assortment of filaments considered.

C. Variation in J_c and AC Loss

We observe a correlation between roughness and J_c (Fig. 5(b)) that parallels the previously reported variation in J_c with grain size for these strands [8]. We also observe a trend of higher AC loss with increasing interface perimeter length but not waviness or roughness. The grain size may impact properties in multiple ways, including mechanical influences like drawability and intrinsic properties such as the final superconductor flux-pinning behavior. This technique should provide valuable insights into the contribution of grain size to the final performance.

IV. SUMMARY AND CONCLUSION

The open-source code for extracting sequential heights from an interface is available for the community to explore. A method to analyze the interface roughness of a curved interface has been developed, and the procedures described in this paper provide traditional R_a, and R_q values interpreted from the shorter wavelength, and waviness W_a, and W_q from the longer wavelengths. The procedure can be extended to include a full power spectral density (PSD) analysis that could be implemented to develop the amplitude and the spatial frequency of roughness [15], [16], [17].

The procedure developed has been implemented on 12 different Cu-Nb interface samples provided by KAT. A clear pattern emerges of lower roughness for lower initial grain size. In contrast, we did not observe a relationship between grain size and waviness for these samples.

The tools developed here should make it easy to quantify interfacial roughness and measure filament shape uniformity in

Authorized licensed use limited to: Florida State University. Downloaded on June 28,2023 at 15:27:21 UTC from IEEE Xplore. Restrictions apply.

terms of waviness to aid in optimizing the wire cross-section and the effective filament diameter. The technique also applies to higher resolution microscopes such as electron microscopes and other interfaces that impact the performance of superconductors, such as strand surface roughness in cables [18], and uniformity of diffusion barriers [19].

REFERENCES

[1] A. Ballarino et al., "The CERN FCC conductor development program: A worldwide effort for the future generation of high-field magnets," *IEEE Trans. Appl. Supercond.*, vol. 29, no. 5, Aug. 2019, Art. no. 6001709, doi: 10.1109/TASC.2019.2896469.

[2] D. Tommasini et al., "The 16 T dipole development program for FCC," *IEEE Trans. Appl. Supercond.*, vol. 27, no. 4, Jun. 2017, Art no. 4000405, doi: 10.1109/TASC.2016.2634600.

[3] R. W. Heussner, P. J. Lee, P. D. Jablonski, and D. C. Larbalestier, "The influence of niobium and niobium-titanium grain size on the drawing instability of niobium diffusion barriers in niobium-titanium wire," in *Advances in Cryogenic Engineering Materials: Volume 40, Part A*, R. P. Reed, F. R. Fickett, L. T. Summers, and M. Stieg, Eds. Boston, MA, USA: Springer US, 1994, pp. 755–762, doi: 10.1007/978-1-4757-9053-5_96.

[4] S. Hong, M. B. Field, J. A. Parrell, and Y. Zhang, "Latest improvements of current carrying capability of niobium tin and its magnet applications," *IEEE Trans. Appl. Supercond.*, vol. 16, no. 2, pp. 1146–1151, Jun. 2006, doi: 10.1109/TASC.2005.864270.

[5] A. A. Polyanskii et al., "Evidence for highly localized damage in internal tin and powder-in-tube Nb3Sn strands rolled before reaction obtained from coupled magneto-optical imaging and confocal laser scanning microscopy," *Supercond. Sci. Technol.*, vol. 22, no. 9, Aug. 2009, Art. no. 095008, doi: 10.1088/0953-2048/22/9/095008.

[6] S. Balachandran et al., "Fine grained Nb for internal tin Nb_3Sn conductors," *AIP Conf. Proc.*, vol. 1219, no. 1, pp. 216–223, Apr. 2010, doi: 10.1063/1.3402304.

[7] S. Balachandran et al., "Influences of different ECAE routes on filament deformation in Cu Clad Nb composite wires," *IEEE Trans. Appl. Supercond.*, vol. 21, no. 3, pp. 2584–2587, Jun. 2011, doi: 10.1109/TASC.2011.2108630.

[8] D. Smathers, J. Flanigan, J. Kim, and K. Sim, "Niobium rod quality and its impact on the production of Nb_3Sn strand for the Divertor Tokamak Test Facility toroidal coils," *IOP Conf. Ser. Mater. Sci. Eng.*, vol. 1241, no. 1, May 2022, Art. no. 012017, doi: 10.1088/1757-899X/1241/1/012017.

[9] ISO 21920-2:2021(en), "Geometrical product specifications (GPS) – Surface texture: Profile – Part 2: Terms, definitions and surface texture parameters," Dec. 31, 1969. Accessed: Mar. 1, 2023. [Online]. Available: https://www.iso.org/obp/ui/#iso:std:iso:21920:-2:ed-1:v2:en

[10] S. R. Nayak, J. Mishra, and G. Palai, "Analysing roughness of surface through fractal dimension: A review," *Image Vis. Comput.*, vol. 89, pp. 21–34, Sep. 2019, doi: 10.1016/j.imavis.2019.06.015.

[11] S. L. Roux, F. Deschaux-Beaume, T. Cutard, and P. Lours, "Quantitative assessment of the interfacial roughness in multi-layered materials using image analysis: Application to oxidation in ceramic-based materials," *J. Eur. Ceram. Soc.*, vol. 35, no. 3, pp. 1063–1079, Mar. 2015, doi: 10.1016/j.jeurceramsoc.2014.09.027.

[12] M. J. R. Stegmueller, R. J. Grant, and P. Schindele, "Quantification of the interfacial roughness when coating stainless steel onto aluminium by friction surfacing," *Surf. Coatings. Technol.*, vol. 375, pp. 22–33, Oct. 2019, doi: 10.1016/j.surfcoat.2019.06.060.

[13] J. Schindelin et al., "Fiji: An open-source platform for biological-image analysis," *Nature Methods*, vol. 9, no. 7, pp. 676–682, Jul. 2012, doi: 10.1038/nmeth.2019.

[14] D. Nečas and P. Klapetek, "Gwyddion: An open-source software for SPM data analysis," *Central Eur. J. Phys.*, vol. 10, no. 1, pp. 181–188, Feb. 2012, doi: 10.2478/s11534-011-0096-2.

[15] B. N. J. Persson, O. Albohr, U. Tartaglino, A. I. Volokitin, and E. Tosatti, "On the nature of surface roughness with application to contact mechanics, sealing, rubber friction and adhesion," *J. Phys. Condens. Matter*, vol. 17, no. 1, p. R1-R62, Dec. 2004, doi: 10.1088/0953-8984/17/1/R01.

[16] J. M. Elson and J. M. Bennett, "Calculation of the power spectral density from surface profile data," *Appl. Opt.*, vol. 34, no. 1, pp. 201–208, Jan. 1995, doi: 10.1364/AO.34.000201.

[17] T. D. B. Jacobs, T. Junge, and L. Pastewka, "Quantitative characterization of surface topography using spectral analysis," *Surf. Topogr. Metrol. Properties*, vol. 5, no. 1, Jan. 2017, Art. no. 013001, doi: 10.1088/2051-672X/aa51f8.

[18] C. Sanabria, P. J. Lee, W. Starch, A. Devred, and D. C. Larbalestier, "Metallographic autopsies of full-scale ITER prototype cable-in-conduit conductors after full cyclic testing in SULTAN: III. The importance of strand surface roughness in long twist pitch conductors," *Supercond. Sci. Technol.*, vol. 29, no. 7, May 2016, Art. no. 074002, doi: 10.1088/0953-2048/29/7/074002.

[19] K. T. Hartwig, S. Balachandran, S. N. Mathaudhu, R. E. Barber, T. Pyon, and R. B. Griffin, "Interface roughness in copper-tantalum wire and Nb_3Sn superconductor composites," *AIP Conf. Proc.*, vol. 986, no. 1, pp. 325–332, Mar. 2008, doi: 10.1063/1.2900363.

Authorized licensed use limited to: Florida State University. Downloaded on June 28,2023 at 15:27:21 UTC from IEEE Xplore. Restrictions apply.